Journal of Power Sources 238 (2013) 1–10

Contents lists available at SciVerse ScienceDirect

Journal of Power Sources

journal homepage: www.elsevier.com/locate/jpowsour

Nafion-based membrane electrode assemblies prepared from catalyst inks containing alcohol/water solvent mixtures

Trung Truc Ngo [a], T. Leon Yu [a,b,*], Hsiu-Li Lin [a,b]

[a] Department of Chemical Engineering & Materials Science, Yuan Ze University, Chung-Li, Taoyuan 32003, Taiwan
[b] Fuel Cell Center, Yuan Ze University, Chung-Li, Taoyuan 32003, Taiwan

HIGHLIGHTS

- Pt surface area increases with decreasing alcohol content of catalyst solution.
- Pt surface area depends on solubility parameter δ and dielectric constant ε of, catalyst ink solvent.
- Fuel cell performance depends on δ and ε of catalyst ink solvent.

GRAPHICAL ABSTRACT

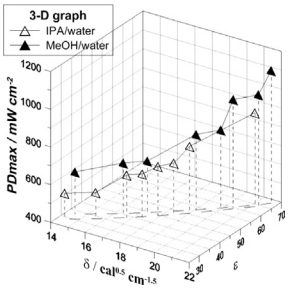

ARTICLE INFO

Article history:
Received 14 January 2013
Received in revised form
5 March 2013
Accepted 12 March 2013
Available online 21 March 2013

Keywords:
Nafion catalyst ink solutions
Platinum catalyst electrodes
Membrane electrode assembly
Proton exchange membrane fuel cell

ABSTRACT

Many researchers have studied the influence on fuel cell (FC) performance of the dielectric constants (ε values) of the dispersion solvents of catalyst ink solutions in the fabrication of Nafion-based gas diffusion electrodes (GDEs). They have reported that Nafion forms colloidal particles in dispersion solvents possessing $\varepsilon = 3-10$, making these solvents suitable for fabricating GDEs with excellent FC performance. In this paper, we study the dependence of both the Nafion ionomer morphology in the catalyst layers and the FC performance of the GDEs on ε and the solubility parameter δ of the alcohol (i.e., methanol and isopropyl alcohol)/water dispersion mixture. The dispersion solvents of the catalyst ink solutions contain 20–100 wt.% alcohol with $23.4 > \delta > 11.3$ and $78.4 > \varepsilon > 19.9$. By plotting the FC performance against the ε and δ values of the alcohol/water dispersion solvent mixture, we demonstrate that the FC performance increases with increasing ε and δ values of the catalyst ink dispersion solvents. ε and δ are determined to be better parameters than the compositions of the solvent mixtures for describing GDE performance.

1. Introduction

Hydrogen with proton exchange membrane fuel cells (PEMFCs) is currently considered as a potential next-generation alternative energy technology because of the high energy density and high abundance of hydrogen in nature. Nafion ionomer is the most widely used polyelectrolyte for proton exchange membrane (PEM) technology, used as the electrolyte binder of the catalyst particles in the catalyst layer (CL), which are the major components of the membrane-electrode assemblies (MEAs) in the PEMFCs [1–6]. A high-performance MEA requires a combination of effective contact at the three-phase boundary, high Pt (platinum) catalyst utilization, sufficient proton conduction, and facile H_2 and O_2 reactant and water product transport to and from the Pt active sites in the CL. The use of Nafion ionomer in the CL increases the three-dimensional zone of catalytic activity. Nafion serves as the

* Corresponding author. Department of Chemical Engineering & Materials Science, Yuan Ze University, Chung-Li, Taoyuan 32003, Taiwan. Tel.: +886 3 4638800x2553; fax: +886 3 4559373.
E-mail address: cetlyu@saturn.yzu.edu.tw (T.L. Yu).

0378-7753/$ – see front matter © 2013 Elsevier B.V. All rights reserved.
http://dx.doi.org/10.1016/j.jpowsour.2013.03.055

physical binder and proton conductor in the CLs; additionally, the molecular interaction between the Pt particles and the Nafion ionomer may play a key role in governing the final microstructure and properties of the CLs [7]. The catalyst ink solutions used for MEA fabrication consist of Pt–C (Pt on carbon powder support), Nafion ionomer, and dispersion solvents. It is the molecular interactions of the Nafion ionomer and the solvents that control the Nafion molecular morphology in solution and thus the final microstructure of Nafion in the CLs. Therefore, the selection of the dispersion solvent for the catalyst ink solution is critical for obtaining an MEA with high performance.

The most common methods for CL fabrication are decal [8], gas diffusion layer (GDL) [9], and membrane-based or catalyst-coated membrane (CCM) [10]. Uchida et al. [9,11,12] and Shin et al. [13] reported that the dielectric constant ε of the dispersion solvent of the Pt–C/Nafion catalyst ink solution determines the state of the Nafion ionomer in solution. It was reported that the Nafion ionomer could be solubilized in organic solvents with $\varepsilon > 10$. However, the Nafion ionomer formed colloidal solutions in organic solvents with $10 > \varepsilon > 3$ and precipitated in solvents with $\varepsilon < 3$. The authors prepared gas diffusion electrodes (GDEs) using the GDL-based method and showed that electrodes prepared form a colloidal form of the catalyst ink exhibited better fuel cell (FC) performance than those prepared from the solution form of the catalyst ink. According to these authors, the colloidal catalyst ink method secured the continuity of the ionomer network and the enlargement of the CL secondary pore structure, resulting in increased proton conductivity, reduced mass transfer resistance, and increased FC performance as a consequence. The effect of the organic dispersion solvents with various values of ε, such as alcohols, ketones, glycols, oxalates, ethers, water/glycol mixtures, butyl acetate/glycerol mixture, alcohol/glycerol mixtures, water/glycerol mixtures, etc., on the CL structure and the fuel cell performance of the MEAs was further studied using the decal [14,15], GDL-based [16,17], and CCM [18,19] processing methods. All of these papers discussed the CL morphology and the fuel cell performance of MEAs based on the ε value of the catalyst ink solution solvent.

It is known that Nafion possesses dual solubility parameters, i.e., $\delta_1 = 9.7$ cal$^{0.5}$ cm$^{-1.5}$ for the hydrophobic perfluorocarbon backbones and $\delta_2 = 17.3$ cal$^{0.5}$ cm$^{-1.5}$ for the hydrophilic sulfonated vinylether side chains [20]. The hydrophobic perfluorocarbon backbones are not compatible with the hydrophilic vinylether side chains in solution; hence, the morphology of the Nafion ionomer in dilute solutions and in the solution casting membranes depends not only on the ε value but also on the δ value of the solvents [21–23]. However, few papers have reported the influence of the δ value of the dispersion solvent used for the catalyst ink solution on the morphology of the Nafion ionomer in CLs and on the FC performance. Alcohol/water solvent mixtures are the most common dispersion solvents used in the preparation of catalyst ink solutions. In a previous work [24], using dispersion solvent mixtures of isopropyl alcohol (IPA)/water ([IPA] = 20–100 wt.%, $\varepsilon \geq 19.9$) for the Pt–C/Nafion ink solutions (where Pt–C is a carbon powder with 38 wt.% Pt particles deposited on its surface), we reported that the morphologies of the Pt–C/Nafion microstructures in the CLs of the GDEs were strongly dependent on the δ and ε values of the dispersion solvents of the catalyst inks. We showed that the Pt electrochemical active surface areas (Pt-ECSAs) of the CLs and the FC performance of the GDEs can be correlated to the δ and ε values of the IPA/water solvent mixtures of the Pt–C/Nafion catalyst ink solutions.

In this work, further investigation of the relationships between the Pt-ECSAs of the CLs and the FC performances of the MEAs with respect to the δ and ε values of the alcohol/water mixture dispersion solvents of the Pt–C/Nafion catalyst ink solutions is performed, using methanol (MeOH)/water solvent mixtures ([MeOH] = 20–100 wt.%; $\delta = 14.5$–21.68 cal$^{0.5}$ cm$^{-1.5}$ and $\varepsilon > 32$). A comparison between the present results with those obtained using IPA/water mixture dispersion solvents (our previous work [24]) is also performed. The wt. ratios of Pt–C/Nafion in the GDEs and CLs of the MEAs were maintained at a fixed value, i.e., Pt–C/Nafion = 2.3/1 by wt. [24].

2. Experimental

2.1. Preparation of the Nafion solutions

A commercial Nafion solution (Du Pont Co., sulfonic acid equivalent weight of Nafion = approximately 1100 g eq.$^{-1}$) containing 20 wt.% of Nafion and 80 wt.% of aliphatic alcohol and water solvent mixture was heated at 60 °C (below T_g = approximately 105 °C of Nafion) under ambient pressure for 1 h and then at 60 °C under vacuum for 48 h to obtain a solid Nafion resin. To prepare the Nafion solutions, the solid Nafion resin was then dissolved in a series of MeOH/water solvent mixtures in which the MeOH concentration was varied from 20 wt.% to 100 wt.%. A total of 8 Nafion solutions (in which the solvent compositions were [MeOH]/[MeOH + water] = 100, 80, 70, 50, 40, 35, 25, and 20 wt.%) were prepared. All of the solutions had a Nafion concentration of 0.6 mg mL^{-1}.

2.2. Transmission electron microscopy (TEM) observations

The morphologies of the Nafion molecules in dilute solutions were observed using a JEM 2100 (HR) TEM at an accelerating voltage of 80 kV. Each Nafion solution, prepared as described in Section 2.1, was processed into an appropriate sample for TEM observation. The procedures were the same as those described in Section 2.4 of our previous work [24].

2.3. Preparation of the catalyst ink solutions

The same solid Nafion resin prepared as described in Section 2.1 was used for preparation of the catalyst ink solutions. The Pt–C catalyst (38 wt.% Pt content, Johnson Matthey), Nafion, and MeOH/water solvent mixtures with MeOH concentrations ranging from 20 wt.% to 100 wt.% were mixed by sonication for at least 48 h at room temperature to obtain homogeneous ink solutions. The wt. ratio of Pt–C/Nafion was 2.3/1, and the concentration of [Pt–C + Nafion] in each ink solution was approximately 1.0 wt.%. A total of 8 catalyst ink solutions (in which the solvent compositions were [MeOH]/[MeOH + water] = 100, 80, 70, 50, 40, 35, 25, and 20 wt.%) were prepared.

2.4. Pt-ECSA studies for the Pt–C/Nafion GDEs

The catalyst ink solutions containing the various concentrations of MeOH, prepared as described in Section 2.3, were used for preparation of the Pt–C/Nafion GDE samples for the Pt-ECSA studies. The catalyst ink solution was sprayed onto a GDL (10BC carbon paper, SGL Co.) using an ultrasonic spray coating system (Sono Tek Co., NY). The Pt-ECSA measurement of each GDE sample was carried out using cyclic voltammetry (CV; CH1611C Electrochemical Analyzer, CH Instruments). The detailed procedures for the GDE preparations and Pt-ECSA measurements were the same as those described in Section 2.6 of our previous work [24].

2.5. Field emission scanning electron microscopy (FESEM) investigations of the Pt–C/Nafion GDEs

The same samples as those prepared in Section 2.4 for the Pt-ECSA measurements were used for the FESEM observations, which were performed with a JEOL JSM-6701F operated at 10 kV.

Table 1
Solubility parameters δs and dielectric constants εs of, methanol (MeOH)/water solvent mixtures.

MeOH/[MeOH + water]		δ ($cal^{0.5}$ $cm^{-1.5}$)	ε
(wt ratio)	(mol ratio)		
0	0	23.4	78.4
0.20	0.12	21.7	67.7
0.25	0.16	21.3	65.1
0.35	0.23	20.4	60.2
0.40	0.27	20.0	57.8
0.50	0.36	19.1	53.1
0.70	0.46	17.3	44.3
0.80	0.69	16.4	40.3
1.00	1.00	14.5	32.7
Nafion	$\delta_1 = 9.7$ $cal^{0.5}$ $cm^{-1.5}$ $\delta_2 = 17.3$ $cal^{0.5}$ $cm^{-1.5}$		

2.6. Preparation of the MEAs

Nafion-212 membranes (Du Pont) were used to fabricate the MEAs. Eight Pt–C/Nafion catalyst ink solutions with methanol/water solvent mixtures containing 100, 80, 70, 50, 40, 35, 25, and 20 wt.% MeOH were used for the anode and cathode CL fabrications. The CL fabrication and MEA preparation procedures were the same as those for the GDEs, as described in Section 2.4 of this work and in Section 2.8 of our previous paper [24]. The active area of each electrode was 3.5 × 3.5 cm^2. The final wt. ratio of [Pt–C]/[Nafion solid resin] on the GDL was approximately 2.3/1, and the Pt loadings on the anode and cathode CLs were 0.2 mg cm^{-2} and 0.4 mg cm^{-2}, respectively.

2.7. Unit fuel cell tests and impedance measurements

The performances (the *i*–V curves and AC-impedances) of the PEMFC unit cells of the MEAs, prepared as described above (*Preparation of the MEAs*), were tested under ambient pressure using a Model 850e Fuel Cell Test System (Scribner Associates, Inc.). All of the anode, cathode, and cell temperatures were 80 °C. Both the input H_2 and O_2 flow rates were 500 mL min^{-1} with 100% relative humidity (RH). The potential state for the AC-impedance measurements was kept at $i = 1000$ mA cm^{-2}, and the scanning frequency range was from 10^4 Hz to 0.1 Hz.

3. Results and discussion

3.1. Solubility parameters and dielectric constants of the solvents

Nafion is known to be composed of two incompatible chemical structures, i.e., a hydrophobic perfluorocarbon backbone and hydrophilic sulfonated vinylether side chains [1,20,27,28]. It has been shown that the Nafion molecular morphology in dilute solutions is strongly dependent on the δ and ε values of the solvents [23,24]. Before discussing the morphology of Nafion in both the alcohol/water mixture solutions and the CLs prepared using the alcohol/water solvent mixtures, we briefly describe our estimations of the δ and ε values of the MeOH/water mixture and IPA/water solvent mixtures containing various wt. ratios of alcohol. In our previous work, we calculated the δ and ε values of the IPA/water solvent mixtures using Eqs. (1) and (2), respectively [23–26]. In this study, using the same method, we calculated the δ and ε values of the alcohol/water solvent mixtures. Tables 1 and 2 summarize the calculated δ and ε values of the MeOH/water and IPA/water solvent mixtures, respectively. The dual solubility parameters $\delta_1 = 9.7$ $cal^{0.5}$ $cm^{-1.5}$ and $\delta_2 = 17.3$ $cal^{0.5}$ $cm^{-1.5}$ of Nafion [20] are also listed in Table 1.

$$\delta_m = \left[E_{coh,m}/V_m\right]^{1/2} = \left[\left(\sum X_i E_{coh,i}\right)\Big/\left(\sum X_i V_i\right)\right]^{1/2} \quad (1)$$

$$\rho_m = \sum X_i \rho_i = \sum X_i \varepsilon_i^{1/2} M_i \quad (2a)$$

$$\varepsilon_m = \left[\rho_m/\left(\sum X_i M_i\right)\right]^2 \quad (2b)$$

where δ_m is the δ of the solvent mixture, $E_{coh,m}$ is the cohesive energy of the solvent mixture, V_m is the molar volume of the solvent mixture, X_i is the molar ratio of solvent-*i*, $E_{coh,i}$ is the cohesive energy of solvent-*i*, V_i is the molar volume of solvent-*i*, ρ_m is the molar dielectric polarization of a solvent mixture, ρ_i is the molar dielectric polarization of solvent-*i*, ε_m is the ε of the solvent mixture, ε_i is the dielectric of solvent-*i*, and M_i is the molecular weight of solvent-*i*.

3.2. TEM studies of Nafion morphology in dilute Nafion-methanol/water solutions

The dilute Nafion MeOH/water solutions ([MeOH] = 0.2, 0.25, 0.35, 0.40, 0.50, 0.70, 0.80, and 1.0 wt.%) were frozen at −190 °C and then dried under vacuum at −130 °C on the surface of TEM copper grid samples to fix the morphology of the Nafion molecules similarly to those in dilute solution for TEM observation. In Fig. 1, we present the TEM micrographs (magnitudes 2×10^4 and 1×10^5) of the Nafion molecular morphologies for 5 frozen samples of 0.6 mg mL^{-1} Nafion MeOH/water solutions containing 20, 35, 50, 70, and 100 wt.% of MeOH. The TEM micrographs of the samples prepared from MeOH/water solvent mixtures containing 25, 40, and 80 wt.% MeOH were similar to those prepared from MeOH/water solvent mixtures containing 20, 35, and 70 wt.% MeOH; hence, they are not shown here. These TEM micrographs clearly show that small, compact primary Nafion particles (as indicated by the red dashed curves shown in the TEM micrographs of Fig. 1a′–e′) are present in solution. These compact primary particles tend to form secondary loose aggregated particles (as indicated by the dashed rectangles shown in the TEM micrographs of Fig. 1a–e). These small, compact particles have rod-like structures with rod lengths of approximately 50–80 nm, tending to aggregate to form larger, loose secondary clusters with sizes of approximately 110–270 nm when the MeOH concentration in the MeOH/water solvent mixture is approximately 20–80 wt.%. The structure of the primary aggregated particles changed from rod-like to coiled-like as the MeOH concentration of the MeOH/water solvent mixture was increased from 80 wt.% to 100 wt.% (i.e., a pure methanol solvent). Because the Nafion fluorocarbon backbones and the vinylether sulfonic acid side chains are not compatible [23,24,27,28], aggregation of the Nafion molecules and the formation of compact primary aggregated particles in solution cannot be

Table 2
Solubility parameters δs and dielectric constants εs of, isopropyl alcohol (IPA)/water solvent mixtures.

IPA/[IPA + water]		δ ($cal^{0.5}$ $cm^{-1.5}$)	ε
(wt ratio)	(mol ratio)		
0	0	23.4	78.4
0.2	0.07	21.2	63.6
0.4	0.17	19.0	50.4
0.45	0.20	18.5	47.3
0.50	0.23	17.9	44.3
0.55	0.27	17.4	41.5
0.60	0.31	16.8	38.7
0.70	0.41	15.6	33.4
0.80	0.55	14.4	28.5
1.00	1.00	11.8	19.9

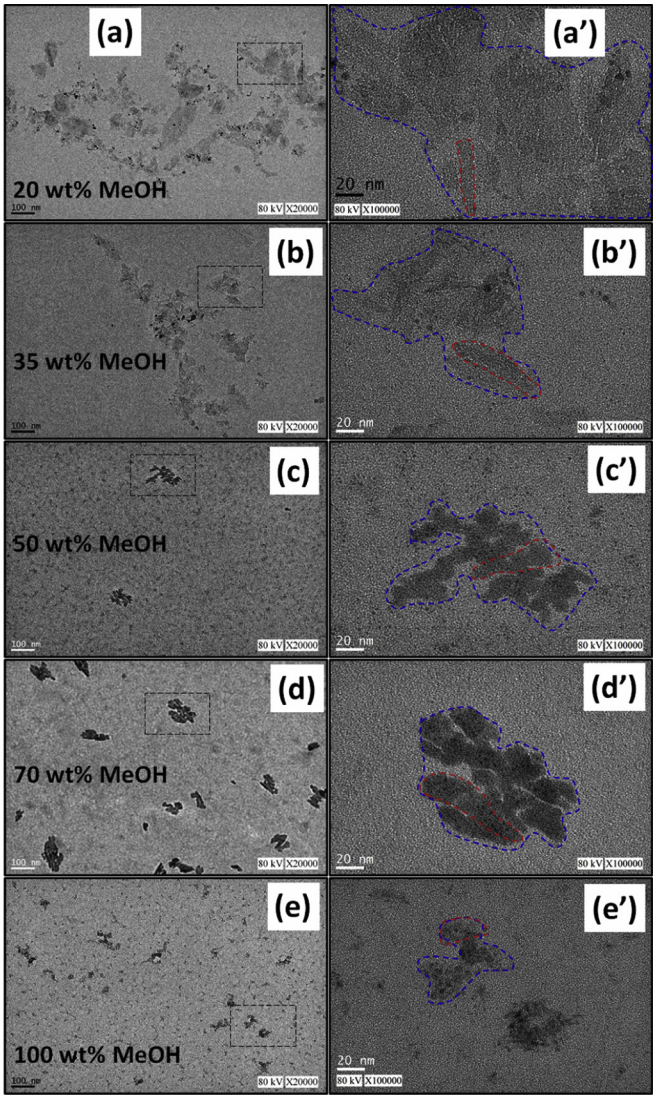

Fig. 1. TEM micrographs of Nafion molecular morphology in 0.6 mg mL^{-1} Nafion methanol (MeOH)/water solutions after freeze drying. Figs. a′–e′ (magnitude × 10^5, scale bar 20 nm) are the enlarged graphs of the secondary aggregated particles inside the dashed rectangles of Figs. a–e (magnitude $\times 2 \times 10^4$, scale bar 100 nm). The red and blue dashed curves indicate the primary and secondary aggregated particles, respectively. The MeOH concentrations in the MeOH/water solvent mixtures are: (a, a′) 20 wt.%; (b, b′) 35 wt.%; (c, c′) 50 wt.%; (d, d′) 70 wt.%; (e, e′) 100 wt.%. (For interpretation of the references to colour in this figure legend, the reader is referred to the web version of this article.)

attributed to interactions among the backbones and side chains; in contrast, the aggregation is attributed to associations either via the inter-polymer fluorocarbon backbone interactions or via the inter-ionic interactions of the negatively charged $-SO_3^-$ groups of two polymer side chains with positively charged H_3O^+ ions, i.e., $\sim SO_3^- \cdots [H_3^+O] \cdots {}^-O_3S \sim$. Because of the negative charge repulsion of the side chain vinylether $-SO_3^-$ groups, the inter-polymer fluorocarbon backbone associations dominate the formation of Nafion compact primary aggregated particles, which depend on the compatibility of the solvent with the Nafion fluorocarbon backbones, i.e., a measure of how small the difference $|\delta_s - \delta_1|$ is, where δ_s is the δ value of the solvent. Association of the Nafion fluorocarbon backbones in solution causes the fluorocarbon backbones to be located within the primary aggregated particles, where the negatively charged vinylether sulfonate chains surround the surfaces of the primary aggregated particles [29,30]. Thus, the inter-polymer vinylether sulfonate interactions, i.e., $\sim SO_3^- \cdots [H_3^+O] \cdots {}^-O_3S \sim$, dominate the association of the compact primary particles with the formation of loose secondary clusters. The inter-polymer vinylether sulfonate side chain interactions depend on the compatibility of the solvent with the vinylether sulfonate side chains (i.e., a measure of how small the difference $|\delta_s - \delta_2|$ is) and on the ε value of the solvent, which determines the degree of dissociation of the $-SO_3H$ groups. Consequently, the negative charge content of each Nafion compact primary aggregated particle is also determined.

Fig. 2a and b presents TEM micrographs from which the dimensions of the particle long axes and widths of the Nafion compact primary and loose secondary aggregates were estimated for the dilute MeOH/water solutions. The sizes (or rod lengths) of the primary compact particles increase from approximately 50 nm to approximately 80 nm as the MeOH concentration of the solvent mixture is increased from 20 wt.% to 70 wt.%, followed by a decrease from approximately 80 nm to approximately 30 nm as the MeOH concentration of the MeOH/water solvent mixture is further increased from 70 wt.% to 100 wt.% (Fig. 2a). The micrographs also show that the sizes of the loose secondary aggregated clusters and the number of small, compact primary particles within each loose secondary cluster decrease with increasing MeOH concentration in the solvent mixture (Figs. 1 and 2b).

The variations in the Nafion molecular morphology in dilute solution as observed in the TEM studies can be explained based on the δ and ε values of the solvents. From Table 1, we know that δ_s of the MeOH/water solvent mixture increases from 17.3 $cal^{0.5}$ $cm^{-1.5}$ to 23.4 as the wt. ratio of MeOH in the solvent mixture decreases from 70 wt.% to 0 wt.%. The solvent mixtures containing 0.0–70.0 wt.% of MeOH have $\delta_s \geq \delta_2 = 17.3$ $cal^{0.5}$ $cm^{-1.5}$ of the vinylether side chains of Nafion, and the δ_s are significantly larger than the $\delta_1 = 9.7$ $cal^{0.5}$ $cm^{-1.5}$ of the perfluorocarbon backbone of Nafion. One expects that the Nafion primary aggregated particle sizes should increase when the wt. ratio of MeOH in the MeOH/water solvent mixtures decreases from 70 wt.% to 0 wt.% because of an increase in the difference $|\delta_s - \delta_1|$ with the decreasing MeOH concentration of the MeOH/water solvent mixtures. However, the increase in the ε value of the MeOH/water solvent mixture following the decreased MeOH concentration of the solvent mixture results in an increase in the degree of the dissociation of the $-SO_3H$ groups of the vinylether side chains into the negatively charged $-SO_3^-$ groups, which increase the effect of charge repulsion among the Nafion molecules and decrease the Nafion primary aggregated particle sizes. As the MeOH concentration in the MeOH/water solvent mixture is increased from 70 wt.% to 100 wt.%, the δ_s of the solvent mixture decreases from 17.3 $cal^{0.5}$ $cm^{-1.5}$ to 14.5 $cal^{0.5}$ $cm^{-1.5}$, approaching the $\delta_1 = 9.7$ $cal^{0.5}$ $cm^{-1.5}$ of the perfluorocarbon backbone. This result indicates that the solvent mixture becomes more compatible with the Nafion perfluorocarbon backbone with increasing MeOH concentration in the solvent. The improvement in the compatibility of the solvent mixture with the perfluorocarbon backbone reduces the Nafion primary perfluorocarbon backbone aggregation tendency; therefore, the primary aggregated particle size decreases when the MeOH concentration of the solvent mixture is increased from 70 wt.% to 100 wt.%.

In Fig. 2a and b, we also show the TEM estimated particle long axis lengths and wide axis widths of the Nafion compact primary and loose secondary aggregates, respectively, as found in the dilute IPA/water solutions of our previous work [24]. We found that the trends in the variations of the Nafion primary and secondary aggregate particle sizes with respect to the alcohol concentration of the solvent mixtures were similar in these two alcohol/water mixtures. However, for the solvent mixtures with the same alcohol concentrations, the particle sizes of the Nafion aggregates in the MeOH/water solution

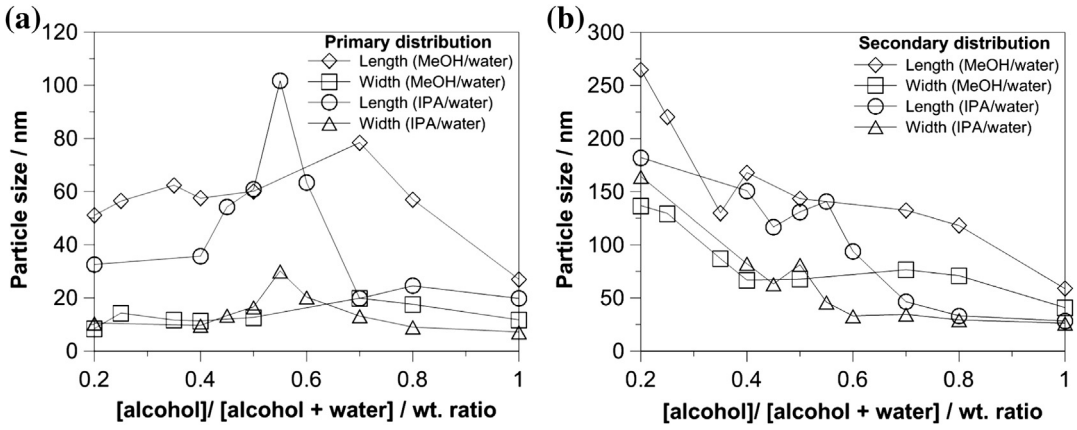

Fig. 2. Variations of Nafion (a) primary aggregated and (b) secondary aggregated particle sizes versus alcohol concentration of the alcohol/water solvent mixtures. (◇) Nafion particle length in methanol (MeOH)/water solvent mixtures; (□) Nafion particle width in MeOH/water mixture solvents; (○) Nafion particle length in isopropyl alcohol (IPA)/water solvent mixtures; (△) Nafion particle width in IPA/water solvent mixtures. The Nafion aggregated particle sizes in IPA/water solutions were estimated from the TEM micrographs shown in Ref. [24].

mixtures were larger than those in the IPA/water solution mixtures. In our previous work, we demonstrated that the morphology of the Nafion molecules in the dilute IPA/water solutions can be interpreted using the δ and ε values of the solvents. Therefore, it is important to study the solvent δ and ε dependences, rather than the alcohol concentration dependence, of the Nafion aggregate particle sizes in the alcohol/water solvent mixtures. Fig. 3a and b present the three-dimensional plots of the particle long axis lengths of the Nafion primary compact aggregates and secondary loose aggregates, respectively, versus the δ and ε values of the MeOH/water and IPA/water solvent mixtures. The dashed lines vertically projected from the data points to the δ and ε planes indicate the lengths of the particle long axes. Although the Nafion aggregates had larger particle sizes in the MeOH/water solvent mixtures than in the IPA/water solvent mixtures, these plots show that the Nafion particles had similar particle sizes when the solvent mixtures had similar δ and ε values, suggesting that the Nafion aggregate particle sizes depend on the δ and ε values of the alcohol/water solvent mixtures, regardless of whether the alcohol is MeOH or IPA. It is interesting to note that, in both the MeOH/water and IPA/water solution mixtures, the Nafion polymers have the largest primary aggregate particle sizes at $\delta_s = \sim 17.3\ \text{cal}^{0.5}\ \text{cm}^{-1.5}$ and $\varepsilon = \sim 42$; these values are related to the alcohol concentrations of the solvent mixtures, particularly those containing 70 wt.% of MeOH and 55 wt.% of IPA. The value of $\delta_s = \sim 17.3\ \text{cal}^{0.5}\ \text{cm}^{-1.5}$ is close to the $\delta_2 = \sim 17.3\ \text{cal}^{0.5}\ \text{cm}^{-1.5}$ of the Nafion vinylether side chains.

3.3. Pt-ECSAs of the Pt–C/Nafion GDEs

The CL of the GDE consists of both Pt–C and Nafion ionomer. The Nafion ionomer extends through the Pt three-dimensional reaction zone and increases the catalyst utilization. The presence of the Nafion ionomer aids proton transport in the CLs; however, overloading of Nafion in the CLs results in high shielding of the Pt particles by the Nafion ionomer, retarding the H_2 and O_2 gases in the process of reaching the Pt particles for carrying out electrochemical reaction. Several research groups have evaluated the Nafion ionomer content of CLs using CV analyses and fuel cell tests

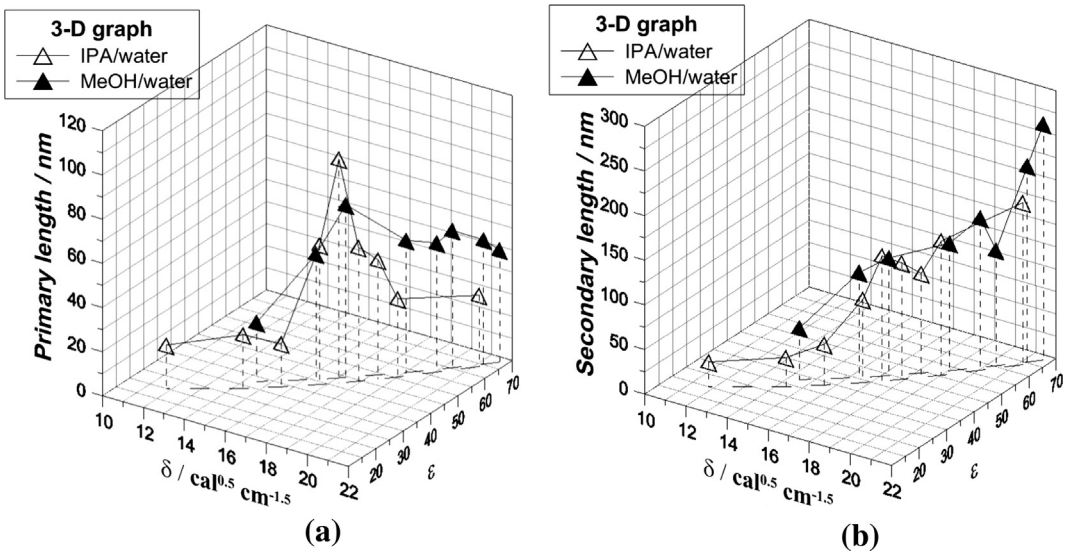

Fig. 3. Three-dimensional plots of the lengths of long axis of (a) Nafion primary rod-like aggregate particles and (b) Nafion secondary loose aggregate particles versus the solubility parameter δ and dielectric constant ε of the methanol (MeOH)/water (▲) and isopropyl alcohol (IPA)/water (△) solvent mixtures. Each vertical dashed line indicates the projection from the datum point to the surface of δ-ε plane and its length is the length of (a) Nafion primary and (b) secondary loose aggregate particle in the solution.

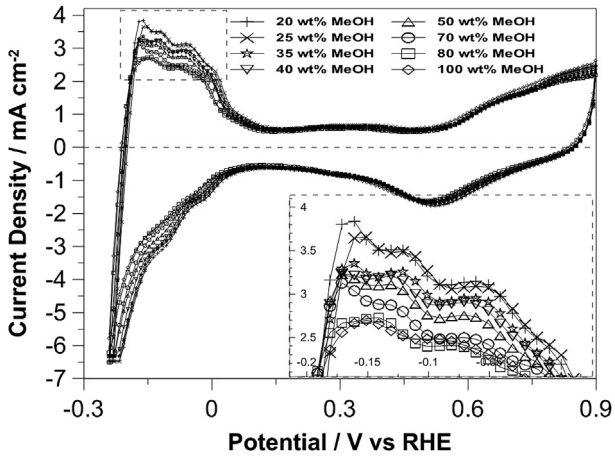

Fig. 4. Cyclic voltammetry (CV) curves of Pt–C/Nafion gas diffusion electrodes (GDEs) prepared from various methanol (MeOH)/water solvent mixtures. wt.% of MeOH in the MeOH/water solvent mixtures: (+) 20 wt.%; (×) 25 wt.%; (☆) 35 wt.%; (▽) 40 wt.%; (△) 50 wt.%; (○) 70 wt.%; (□); 80 wt.%; (◇) 100 wt.%.

[31,32]. Passalacqua et al. [31] and Qi et al. [32] reported an optimum Nafion content of approximately 30–33 wt.% in CLs. In this study, all of the catalyst ink solutions were prepared with a fixed [Pt–C]/[Nafion] wt. ratio of 2.3/1 (see Section 2.3). Therefore, the Nafion content in the CL of each sample was fixed at approximately 30 wt.%. The Pt-ECSAs of the Pt–C/Nafion GDEs prepared from the MeOH/water solutions containing 20–100 wt.% of MeOH were investigated using CV in deaerated 0.5 M H_2SO_4 solution. Fig. 4 shows the cyclic voltammograms of these electrodes recorded at room temperature. The Pt-ECSA of each sample was calculated from the charge measurements collected in the hydrogen adsorption/desorption region, assuming a value of 210 mC cm^{-2} for the adsorption of a hydrogen monolayer [33–35]. The calculated Pt-ECSA data of these GDEs were plotted against the [MeOH]/[MeOH + water] wt. ratios of the solvent mixtures of the catalyst ink solutions (Fig. 5a). In Fig. 5a, we also show the Pt-ECSA data of the GDEs prepared using IPA/water solvent mixtures, which were also reported in our previous paper [24]. These results demonstrate that the Pt-ECSAs of these two series of GDEs decrease with increasing alcohol content of the alcohol/water solvent mixture of the catalyst inks. However, the GDEs prepared using the MeOH/water solvent mixtures had a larger Pt-ECSA than those prepared using the IPA/water solvent mixtures when the alcohol concentration of the solvent mixture was larger than 40 wt.%. As the alcohol concentration of the solvent mixture was further decreased below 40 wt.%, the Pt-ECSAs of these two series of GDEs approached each other. In Fig. 3b, we show that the sizes of the Nafion polymer secondary aggregated particles depend on the δ and ε values of the alcohol/water solvent mixtures. Therefore, the morphology of the Nafion thin film, and thus that of the Pt-ECSA of the CL of the GDE, also should depend on the δ and ε values of the alcohol/water solvent mixtures of the catalyst ink solutions. In Fig. 6, we plot the three-dimensional graphs of the Pt-ECSA data against the δ and ε values of the alcohol/water solvent mixtures. It is interesting to note that the GDEs had similar Pt-ECSA values when prepared using the alcohol/water solvent mixtures with similar δ and ε values, regardless of whether the alcohol was IPA or MeOH.

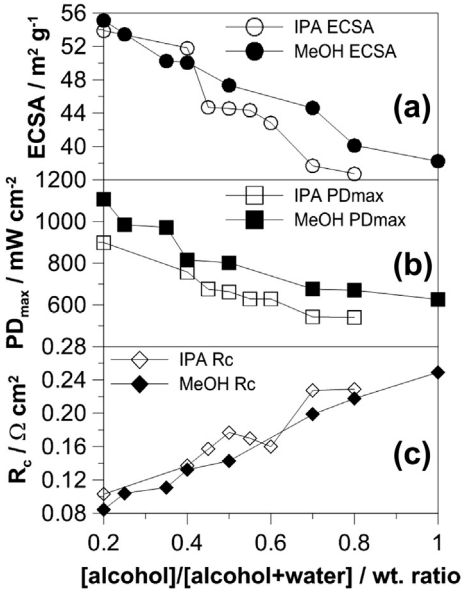

Fig. 5. Plots of (a) cyclic voltammetry (CV) test Pt electrochemical active surface area (Pt-ECSA) data (○) (●); (b) fuel cell test maximum power density (PD_{max}) data (□) (■); (c) catalyst layer (CL) impedance cathode charge transfer resistance (R_c) data (◇) (◆) versus the [alcohol]/[alcohol + water] wt. ratio of the solvent mixtures of the Pt–C/Nafion catalyst ink solutions. (○; □; ◇) catalyst inks prepared from isopropyl alcohol (IPA)/water solvent mixtures; (●; ■; ◆) catalyst inks prepared from methanol (MeOH)/water solvent mixtures.

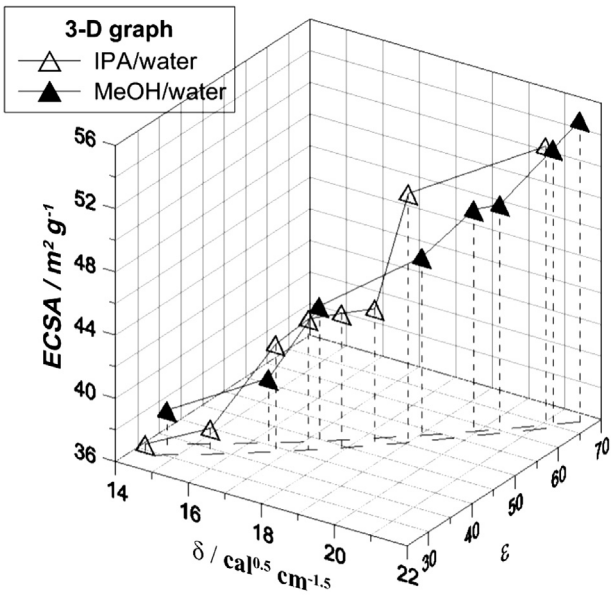

Fig. 6. Three-dimensional plots of the Pt electrochemical active surface areas (Pt-ECSAs) of the gas diffusion electrodes (GDEs) against the solubility parameter δ and dielectric constant ε values of the alcohol/water solvent mixtures of the Pt–C/Nafion catalyst ink solutions. (▲) methanol (MeOH)/water solvent mixtures; (△) isopropyl alcohol (IPA)/water solvent mixtures.

3.4. Morphology of the Pt–C/Nafion layer of the GDEs

Further investigation of the influence of the alcohol/water solvent mixture composition used in the Pt–C/Nafion catalyst ink solutions on the morphology of the Pt–C/Nafion CLs was carried out using FESEM. The GDE samples used in the FESEM observations were the same as those used in the CV Pt-ECSA studies. Fig. 7 shows the FESEM micrographs (magnitude × 10^3) of the GDEs prepared from the MeOH/water solvent mixtures containing various MeOH concentrations. These micrographs show that micro-voids with sizes of approximately 1–5 μm were present in the Nafion/Pt–C thin film and that both the sizes and the number of micro-voids increased and the surface of the CL became more rough with

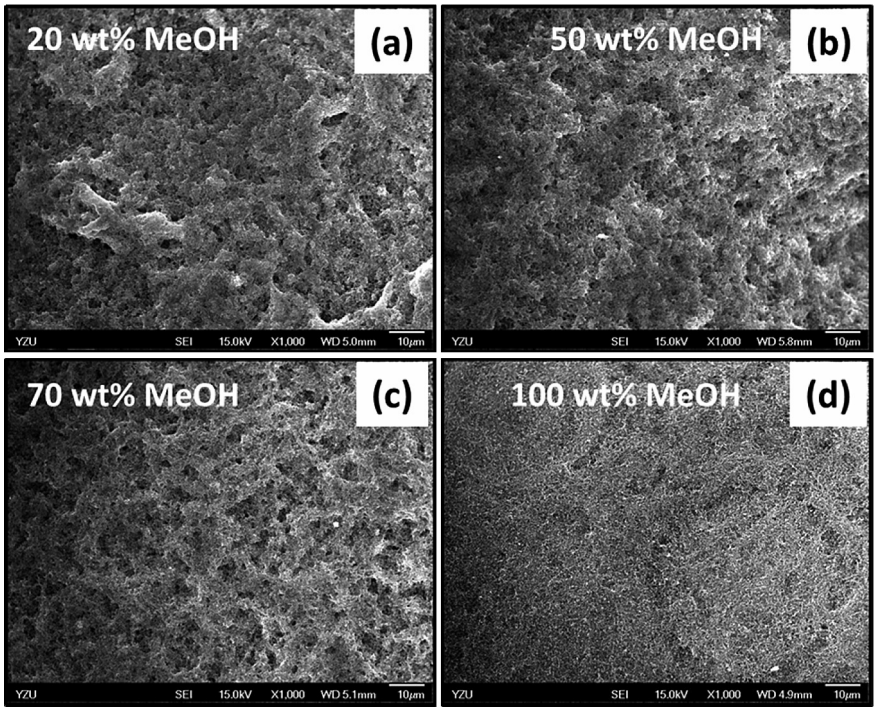

Fig. 7. Field emission scanning electron microscopy (FESEM) micrographs ($\times 10^3$; the scale bar is 10 μm) of the Pt–C/Nafion layer on the surface gas diffusion layer (GDL). [Pt–C]/[Nafion] = 2.3/1 by wt. The methanol (MeOH) concentrations of the Pt–C/Nafion catalyst ink solutions are: (a) 20 wt.%; (b) 50 wt.%; (c) 70 wt.%; (d) 100 wt.% MeOH.

decreasing MeOH concentration of the solvent mixture of the catalyst ink solutions. The micro-voids of the GDEs facilitate the fuel H_2 and O_2 gases in reaching the Pt catalyst particles, allowing the electrochemical reactions in the MEAs to proceed and thereby improving the Pt-ECSA of the GDEs. Therefore, the FESEM data in Fig. 7 are consistent with the CV test Pt-ECSA data presented in Figs. 4 and 5a.

In our previous work [24], we used FESEM to investigate the morphologies of Pt-Nafion CLs of GDEs prepared from IPA/water solvent mixtures containing 20–80 wt.% of IPA. These results showed that the Pt particles were dispersed on the surfaces of the carbon supports with some Pt particles shielded by the Nafion thin film layer; additionally, it was demonstrated that the number of visible Pt particles (i.e., the un-shielded Pt particles) on the surfaces of the carbon powder supports decreased with increasing IPA concentration of the IPA/water solvents used in the Pt–C/Nafion catalyst ink solutions. Similar results were also obtained for GDEs prepared from MeOH/water solvent mixtures containing 20–100 wt.% MeOH, i.e., the number of visible Pt particles (or unshielded Pt particles) on the surfaces of the carbon powder supports decreased with increasing MeOH concentration of the MeOH/water solvents used in the Pt–C/Nafion catalyst ink solutions. Here, we show the morphologies of the Pt-Nafion CLs of the GDEs prepared from the MeOH/water solvent mixtures in comparison with those prepared from the IPA/water solvent mixtures. Fig. 8 shows the FESEM micrographs of the Pt–C/Nafion thin layers of the GDEs, as prepared from Pt–C/Nafion-alcohol/water ink solutions with solvents containing 20, 50, and 80 wt.% of MeOH (the present work) and 20, 50, and 80 wt.% of IPA (the previous work [24]). These micrographs clearly show the carbon powder supports (the gray particles with diameters of approximately 60–80 nm) with Pt particles (the bright spots with diameters less than 5 nm) dispersed on their surfaces. These micrographs show that the number of visible Pt particles on the surfaces of the carbon powder supports decreases with increasing alcohol concentration of the alcohol/water solvents from 20 wt.% to 50 wt.% and to 80 wt.% in the catalyst ink solutions. However, Fig. 8 shows that the number of visible Pt particles in the GDEs prepared from the MeOH/water solvent mixtures is larger than that of the GDEs prepared from the IPA/water solvent mixtures at the same alcohol concentrations, especially when the alcohol concentration of the solvent mixtures was above 50 wt.%. These results are quite consistent with the Pt-ECSA data shown in Fig. 5a, which shows that the GDEs prepared from the MeOH/water solvent mixture have a larger Pt-ECSA than those prepared from the IPA/water solvent mixture when the solvent mixtures consist of the same alcohol concentration. As shown in the TEM observation of Section 3.2 (Figs. 1 and 2), the Nafion polymers achieve larger aggregate particle sizes in the MeOH/water solvent mixtures than in the IPA/water solvent mixtures when the alcohol/water solvent mixtures of the catalyst ink solutions have the same alcohol concentration. The larger size and larger negatively charged, rigid aggregated particles caused increased steric hindrance and charged repulsion for the Nafion aggregated particles, preventing smooth contact on the surfaces of the carbon powder supports during deposition. Therefore, a thinner Nafion film with larger voids between the Nafion thin film and the Pt–C particle was formed on the surfaces of the carbon powders. This architecture led to more un-shielded Pt particles in the GDEs prepared from the MeOH/water solvent mixtures than from the IPA/water solvent mixtures for the solvents with the same alcohol concentration.

3.5. PEMFC unit cell tests and impedance studies of the MEAs

The MEAs prepared from the Nafion-212 membrane with the CLs fabricated using MeOH/water solvents consisting of various MeOH concentrations were used for unit fuel cell performance tests at 80 °C with humidified H_2/O_2 gases. Fig. 9 illustrates the fuel cell test i–V (where i is the current density and V is the cell voltage) and i-PD (power density, i.e., PD(V) = V × i(V), where i(V) is the i obtained at a cell voltage V) curves of these MEAs. The maximum power density (PD_{max}; i.e., the largest PD datum of an i-PD curve)

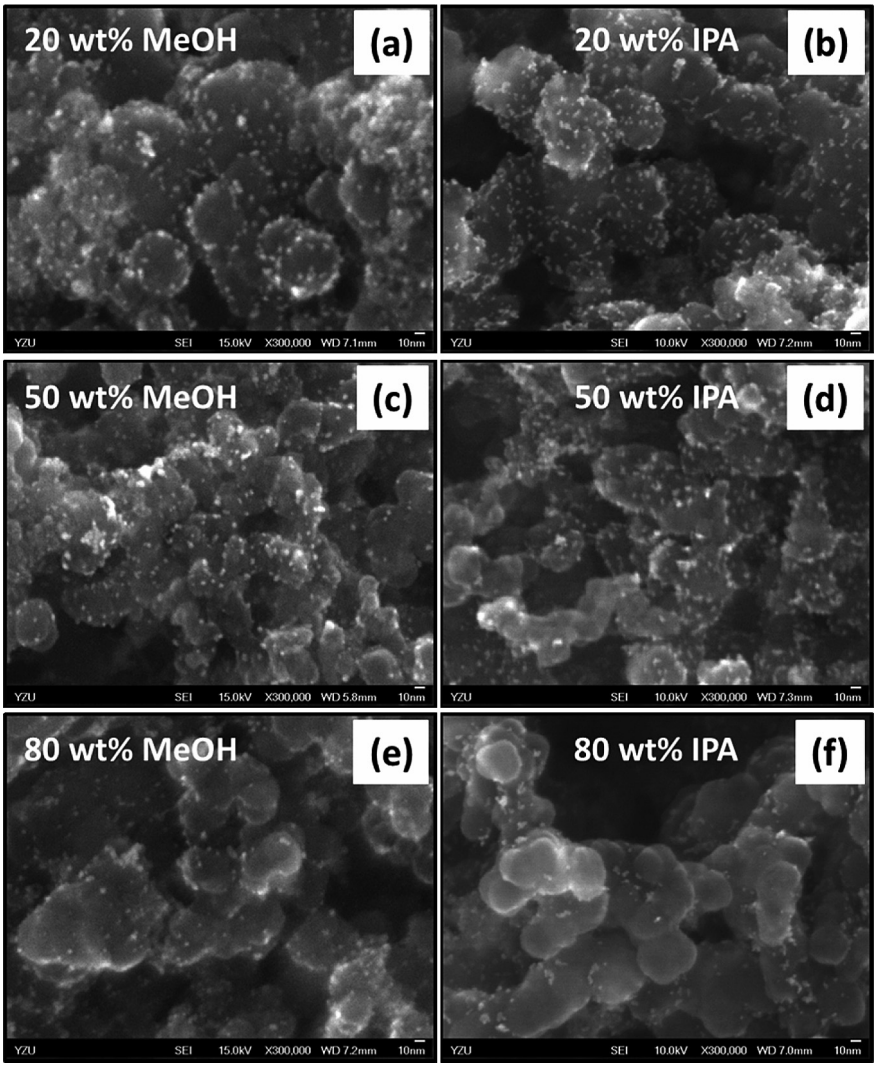

Fig. 8. Field emission scanning electron microscopy (FESEM) micrographs ($\times 3 \times 10^5$; the scale bar is 10 nm) of the Pt–C/Nafion layer on the surface of gas diffusion layer (GDL). The gray particles with diameters of ~60–80 nm are carbon powders, and the bright spots with sizes <5 nm are Pt particles. The alcohol concentrations of the Pt–C/Nafion catalyst ink solutions are: (a) 20 wt.% methanol (MeOH); (b) 20 wt.% isopropyl alcohol (IPA); (c) 50 wt.% MeOH; (d) 50 wt.% IPA; (e) 80 wt.% MeOH; (f) 80 wt.% IPA.

(Table 3) of each MEA was obtained from its *i*-PD data and was plotted against the alcohol concentration of the alcohol/water solvent mixture of the Pt–C/Nafion catalyst ink solutions, as shown in Fig. 5b. In Fig. 5b, we also show the plot of our previous PD_{max} data of the MEAs prepared using the IPA/water solvent mixtures [24]. The results show that the PD_{max} and Pt-ECSA exhibit the same dependence on the alcohol concentration of the alcohol/water solvents of the Pt–C/Nafion catalyst ink solutions. Both the PD_{max} and Pt-ECSA values decrease with increasing alcohol concentration of the alcohol/water solvent mixtures. These data also show that the PD_{max} and Pt-ECSA of the MEAs prepared using the MeOH/water solvent mixtures are larger than those prepared using the IPA/water solvent mixtures when the solvent mixtures consist of the same alcohol concentration. The three-dimensional plots of the PD_{max} data of the MEAs prepared using the MeOH/water and IPA/water solvent mixtures against the δ and ε values of the solvent mixtures are shown in Fig. 10. Similar to the Pt-ECSA data (i.e., Fig. 6), the PD_{max} data of the MEAs prepared from these alcohol/water solvent mixtures have similar PD_{max} values when the alcohol/water solvent mixtures of the catalyst ink solutions have similar δ and ε values.

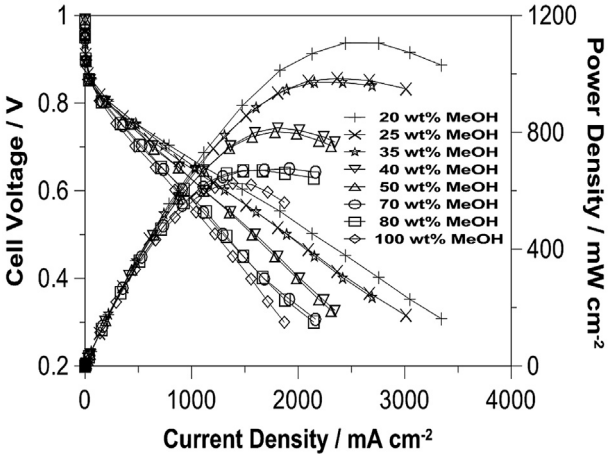

Fig. 9. Polarization curves of PEMFCs with MEAs prepared from catalyst ink solutions containing methanol (MeOH)/water solvent mixtures with various MeOH concentrations. wt.% of MeOH in the MeOH/water solvent mixtures: (+) 20 wt.%; (×) 25 wt.%; (☆) 35 wt.%; (▽) 40 wt.%; (△) 50 wt.%; (○) 70 wt.%; (□); 80 wt.%; (◇) 100 wt.%.

Table 3
Ohmic resistance R_s and cathode charge transfer resistance R_c and fuel cell test maximum power density PD_{max} data of the MEAs prepared from various methanol (MeOH)/water solvent mixtures.

[MeOH]/[MeOH + water] (wt.%)	R_s (10^{-2} Ω cm^2)	R_c (10^{-1} Ω cm^2)	PD_{max} (10^{-1} W cm^{-2})
20	8.0 ± 0.3	0.85 ± 0.04	11.1 ± 0.3
25	8.3 ± 0.3	1.04 ± 0.05	9.9 ± 0.4
35	8.2 ± 0.4	1.11 ± 0.05	9.7 ± 0.2
40	8.9 ± 0.5	1.32 ± 0.07	8.2 ± 0.2
50	8.7 ± 0.5	1.43 ± 0.08	8.0 ± 0.2
70	8.5 ± 0.4	2.0 ± 0.1	6.8 ± 0.3
80	9.1 ± 0.5	2.18 ± 0.09	6.7 ± 0.2
100	9.0 ± 0.5	2.5 ± 0.2	6.3 ± 0.2

AC impedance measurements were also carried out to investigate the resistance of the CLs of the MEAs prepared from the various MeOH/water solvent mixtures. The AC impedance diagrams were simulated using a Randles equivalent circuit consisting of a resistance R_s, representing the total non-electrode cell ohmic resistance in series, with the cathode charge transfer resistance R_c, which is parallel with the capacitive-like element C_d, representative of the electrode double layer [36]. In a fuel cell, the main contribution to R_s (the high frequency resistance) comes from the proton transport resistance of the membrane. Fig. 11 shows the AC impedance diagrams obtained at the constant current i = 1000 mA cm^{-2} for MEAs with Pt–C/Nafion CLs prepared from the MeOH/water solvents containing various concentrations of MeOH. Table 3 lists the R_s and R_c values of the impedance diagrams simulated using the Randles equivalent circuit. Fig. 11 and Table 3 show that the R_s value does not change significantly with the MeOH concentration of the solvents used in the Pt–C/Nafion catalyst ink solutions for MEA CL fabrication because the same membrane (i.e., Nafion-212 membrane) and the same cell and flow field were used in the fuel cell tests. The difference in the fuel cell performance of these MEAs is mainly derived from the difference in the R_c values of the MEAs. The variations in the R_c values of the two series of MEAs prepared from the MeOH/water solvent mixtures in the present work and the IPA/water solvent mixtures in our previous work [24] were plotted against the alcohol concentration of the alcohol/water solvents of the Pt–C/Nafion catalyst ink solutions, as shown in Fig. 5c. These data show that R_c increases with increasing alcohol concentration of the alcohol/water solvent mixture of the catalyst ink solutions. The R_c of the MEA prepared using the IPA/water solvent mixture was larger than that prepared using the MeOH/water solvent mixture when the solvent mixtures had the same alcohol concentration. However, when the R_c values were plotted against the δ and ε values of the alcohol/water solvent mixtures in a three-dimensional graph (Fig. 12), we found that the

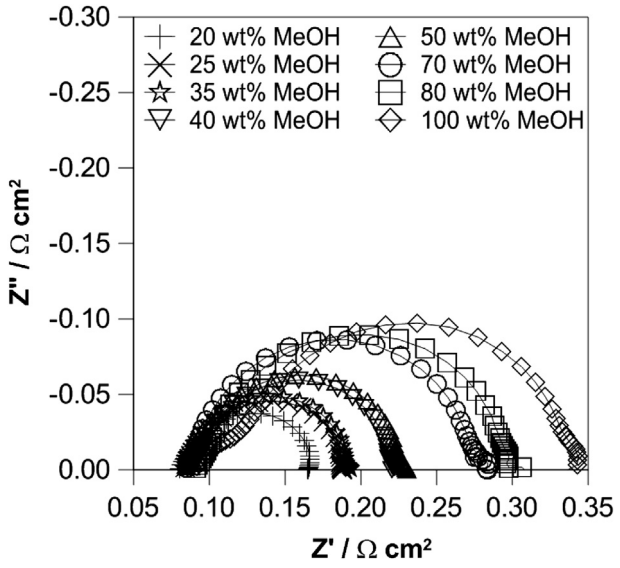

Fig. 11. AC impedance diagrams of MEAs obtained at a constant current i = 1000 mA cm^{-2}. The Pt–C/Nafion catalyst layers (CLs) of the MEAs were prepared from methanol (MeOH)/water solvent mixtures containing various concentrations of MeOH. wt.% of MeOH in the MeOH/water solvent mixtures: (+) 20 wt.%; (×) 25 wt.%; (☆) 35 wt.%; (▽) 40 wt.%; (△) 50 wt.%; (○) 70 wt.%; (□); 80 wt.%; (◇) 100 wt.%.

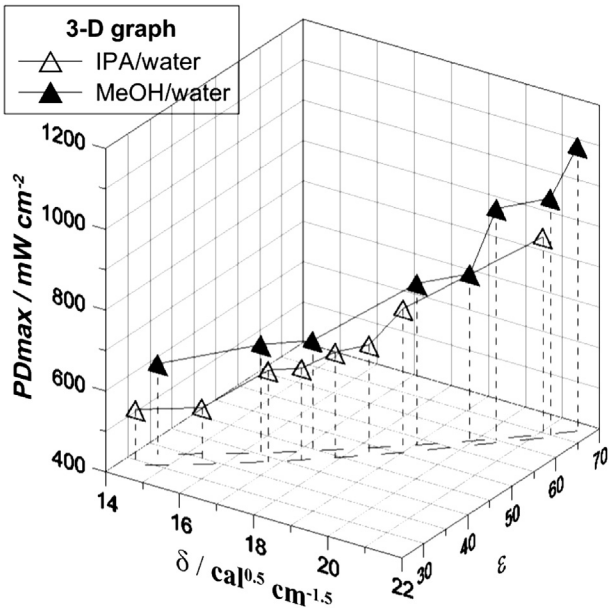

Fig. 10. Three-dimensional plots of the maximum power density (PD_{max}) of the MEAs against the solubility parameter δ and dielectric constant ε values of the alcohol/water solvent mixtures of the Pt–C/Nafion catalyst ink solutions. (▲) methanol (MeOH)/water solvent mixtures; (△) isopropyl alcohol (IPA)/water solvent mixtures.

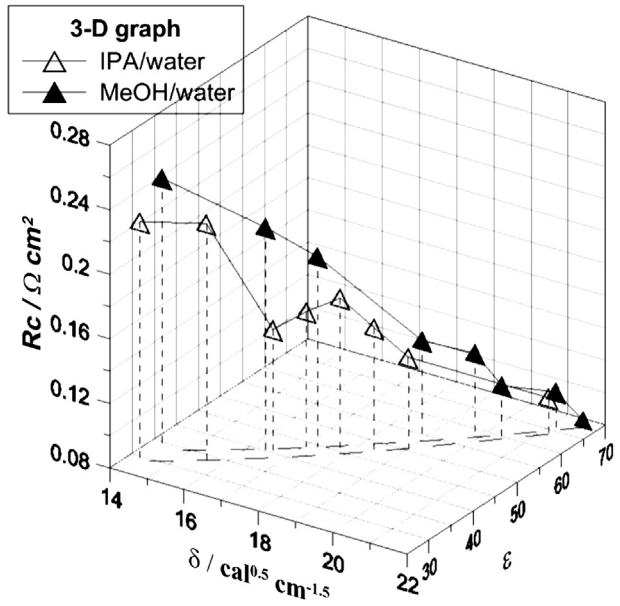

Fig. 12. Three-dimensional plots of the cathode charge transfer resistances (R_cs) of the MEAs against the solubility parameter δ and dielectric constant ε values of the alcohol/water solvent mixtures of the Pt–C/Nafion catalyst ink solutions. (▲) methanol (MeOH)/water solvent mixtures; (△) isopropyl alcohol (IPA)/water solvent mixtures.

MEAs had similar R_c values when the catalyst ink solutions of the MEAs were prepared using the alcohol/water solvent mixtures, i.e., consisting of similar δ and ε values. These results were consistent with the fuel cell PD_{max} data (Figs. 5b and 10).

4. Conclusions

In this study, we investigated the molecular morphology of Nafion in dilute MeOH/water solutions containing 20–100 wt.% of MeOH, the morphology of the Pt–C/Nafion layer in GDEs and the fuel cell performance of MEAs fabricated by the ultrasonic spraying of catalyst ink solutions containing fixed contents of Pt–C and Nafion (Pt–C/Nafion = 2.3/1 by wt.) with MeOH/water solutions containing 20 to 100 wt.% of MeOH. The results reported here were similar to those of Nafion ionomers in dilute IPA/water solvent mixtures, as detailed in our previous work [24]. We demonstrated that the morphologies of Nafion ionomers in alcohol/water solvent mixtures and in the CLs of the GDEs can be described using the δ and ε parameters of the alcohol/water solvent mixtures, rather than the compositions of the alcohol/water solvent mixtures of the catalyst ink solutions. We also showed that the Pt-ECSAs of the GDEs and the fuel cell performances, i.e., the PD_{max} and R_c values, of the MEAs correlate with the morphology of Nafion in the CLs of the GDEs and MEAs. Thus, the δ and ε values of the alcohol/water solvent mixtures of the Pt–C/Nafion ink solutions are better parameters than the compositions of the alcohol/water solvent mixtures of the catalyst ink solutions for describing the Pt-ECSAs, PD_{max}s, and R_cs of the MEAs.

Acknowledgments

The authors would like to thank National Science Council (NSC), Taiwan, ROC for the financial support through grant NSC-96-2221-E-155-041-MY3.

References

[1] W.G. Grot, Nafion as a Separator in Electrolyte Cells. Nafion Product Bulletin, DE, Du Pont Co., Wilmington, DE, 1986.
[2] W.G. Grot, US Patent 4, 453, 991, 1986.
[3] R.B. Moore, C.R. Martin, Anal. Chem. 58 (1986) 2569–2571.
[4] R.B. Moore, C.R. Martin, Macromolecules 21 (1988) 1334–1339.
[5] E.J. Taylor, E.B. Anderson, N.R.K. Vilambi, J. Electrochem. Soc. 139 (1992) L45–L46.
[6] X. Ren, M.S. Wilson, S. Gottesfeld, J. Electrochem. Soc. 143 (1996) L12–L15.
[7] Z. Xie, T. Navessin, X. Zhao, M. Adachi, S. Holdcroft, T. Mashio, A. Ohma, K. Shinohara, ECS Trans. 16 (2008) 1811–1816.
[8] M.S. Wilson, S. Gottsfeld, J. Appl. Electrochem. 22 (1992) 1–7.
[9] M. Uchida, Y. Fukuoka, Y. Sugawara, H. Ohara, A. Ohta, J. Electrochem. Soc. 145 (1998) 3708–3713.
[10] M.S. Wilson, J.A. Valerio, S. Gottesfeld, Electrochim. Acta 40 (1995) 355–363.
[11] M. Uchida, Y. Aoyama, N. Eda, A. Ohta, J. Electrochem. Soc. 142 (1995) 4143–4149.
[12] M. Uchida, Y. Aoyama, N. Eda, A. Ohta, J. Electrochem. Soc. 142 (1995) 463–468.
[13] S.J. Shin, J.K. Lee, H.Y. Ha, S.A. Hong, H.S. Chun, I.H. Oh, J. Power Sources 106 (2002) 146–152.
[14] T.H. Yang, Y.G. Yoon, G.G. Park, W.Y. Lee, C.S. Kim, J. Power Sources 127 (2004) 230–233.
[15] M. Chisaka, E. Matsuoka, H. Daiguji, J. Electrochem. Soc. 157 (2010) B1218–B1221.
[16] R. Fernandez, P. Ferreira-Aparicio, L. Daza, J. Power Sources 151 (2005) 18–24.
[17] D.C. Huang, P.J. Yu, F.J. Liu, S.L. Huang, K.L. Hsueh, Y.C. Chen, C.H. Wu, W.C. Chang, F.H. Tsau, Int. J. Eletrochem. Sci. 6 (2011) 2551–2565.
[18] Z. Xie, X. Zhao, M. Adachi, Z. Shi, T. Mashio, A. Ohma, K. Shinohara, S. Holdcroft, T. Navessin, Energy Environ. Sci. 1 (2008) 184–193.
[19] A. Therdthianwong, P. Ekdharmasuit, S. Therdthianwong, Energy and Fuels 24 (2010) 1191–1196.
[20] R. Yeo, Polymer 21 (1980) 432–435.
[21] S.J. Lee, T.L. Yu, H.L. Lin, W.H. Liu, C.L. Lai, Polymer 45 (2004) 2853–2862.
[22] H.L. Lin, T.L. Yu, C.H. Huang, T.L. Lin, J. Polym. Sci. Part B: Polym. Phys. 43 (2005) 3044–3057.
[23] C.H. Ma, T.L. Yu, H.L. Lin, Y.T. Huang, Y.L. Chen, U.S. Jeng, Y.H. Lai, Y.S. Sun, Polymer 50 (2009) 1764–1777.
[24] T.T. Ngo, T.L. Yu, H.L. Lin, J. Power Sources 225 (2013) 293–303.
[25] E.A. Grulke, J. Brandrup, E.H. Immergut (Eds.), Polymer Handbook, third ed., Wiley Interscience, 1989, pp. VII/519–VII/559.
[26] D.W. Van Krevelen, P.S. Hoftyzer, Properties of Polymers, Elsevier, 1976. (Chapter 7).
[27] M. Fujimura, T. Hashimoto, H. Kawai, Macromolecules 14 (1981) 1309–1315.
[28] M. Fujimura, T. Hashimoto, H. Kawai, Macromolecules 15 (1982) 136–144.
[29] E. Szajdzinska-Pietek, S. Schlick, Langmuir 10 (1994) 1101–1109.
[30] E. Szajdzinska-Pietek, S. Schlick, Langmuir 10 (1994) 2188–2196.
[31] E. Passalacqua, F. Lufrano, G. Squadrito, A. Pattis, L. Giorgi, Electrochim. Acta 46 (2001) 799–805.
[32] Z. Qi, A. Kaufman, J. Power Sources 113 (2003) 37–43.
[33] T.J. Schmidt, H.A. Gasteiger, G.D. Stab, P.M. Urban, D.M. Kolb, R.J. Behm, J. Electrochem. Soc. 145 (1998) 2354–2358.
[34] L. Colombi Ciacchi, A. De Vita, J. Phys. Chem. B 107 (2003) 1755–1764.
[35] D. He, C. Zeng, C. Xu, N. Cheng, H. Li, S. Mu, M. Pan, Langmuir 27 (2011) 5582–5588.
[36] K.R. Cooper, V. Ramani, J.M. Fenton, H.R. Kunz, Experimental Methods and Data Analyses for Polymer Electrolyte Fuel Cells, Scribner Associates, Inc., North Carolina, 2006. Laboratory #5- Impedance spectroscopy of PEM fuel cells.